

Accretion Disks: Limit Cycles and Instabilities

Mario Livio

Space Telescope Science Institute

3700 San Martin Drive, Baltimore, MD 21218

email: mlivio@stsci.edu

Received _____; accepted _____

ABSTRACT

The existing disk instability model for dwarf nova eruptions is reviewed, in the light of recent progress in the understanding of angular momentum transport in accretion disks. It is proposed that the standard lower branch in the “S-curve” in the effective temperature-surface density plane may not exist. Rather, angular momentum transport may be suppressed in quiescence as a result of cooling. The model for superoutbursts is also examined, and it is pointed out that recent simulations strongly support the idea of a thermal-tidal instability.

1. Introduction

The main goal of any discussion of limit cycles in accretion disks is to explain behaviors like dwarf nova eruptions, the outbursts of black-hole x-ray transients, and possibly the outbursts of FU Orionis stars. The first of these is best manifested in the century-long light curve of SS Cyg (e.g. Cannizzo & Mattei 1992; Fig. 1), while the second is extensively reviewed by Chen, Shrader & Livio (1997). At the next level, additional phenomena, like the “standstills” of Z Cam systems (e.g. AAVSO observations, Fig. 2), and the superoutbursts of SU UMa systems (Fig. 3) must be considered.

It is generally believed that all of the above phenomena are related to disk instabilities, with the principal behavior (dwarf nova and x-ray transient eruptions) being explained in terms of a thermal-viscous disk instability model (see e.g. reviews by Cannizzo 1993; Osaki 1996; Lasota & Hameury 1998).

In the present work, I briefly examine some aspects of this and related models and I propose a few possible modifications.

2. The Disk Instability Model

2.1. Steady State

In most of the studies computing limit cycles in standard, thin accretion disks, the conservation equations are written by averaging over the disk thickness. For dwarf nova systems these equations take the form (e.g. Pringle 1981):

mass conservation

$$2\pi R\Sigma(-V_R) = \dot{M} \tag{1}$$

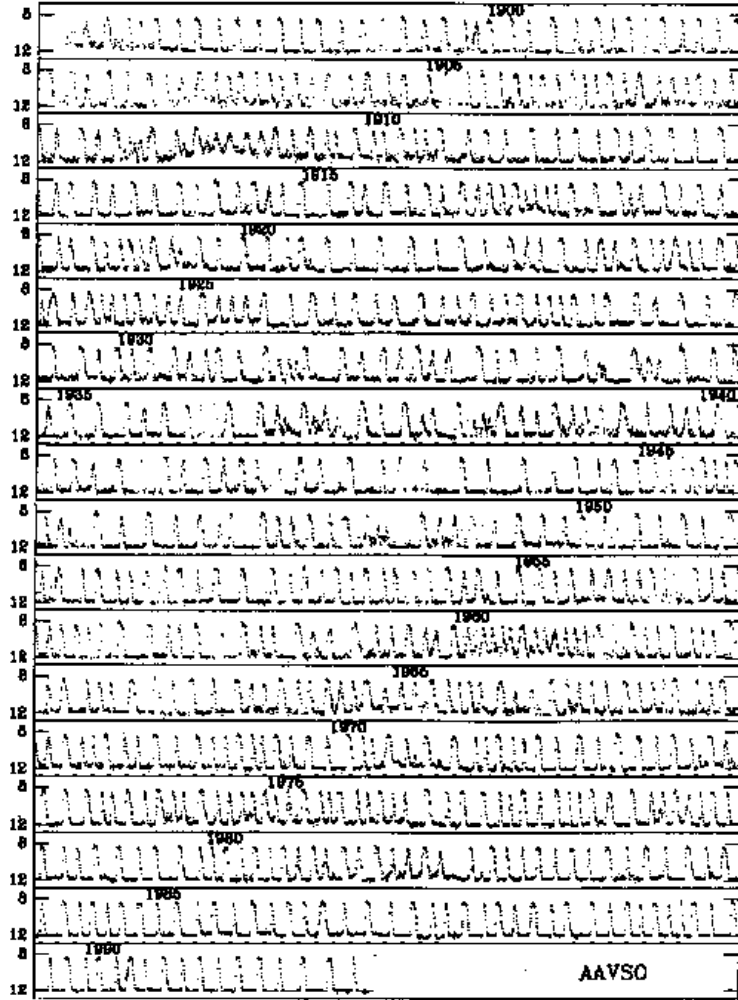


Fig. 1.— The light curve of SS Cyg on the basis of AAVSO observations (from Cannizzo & Mattei 1992).

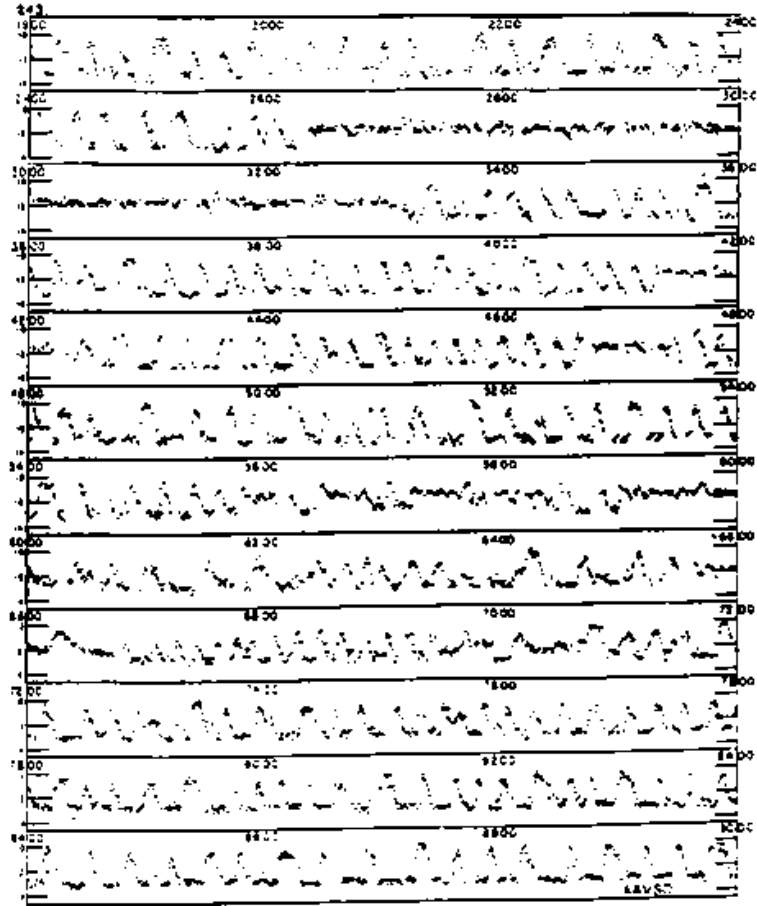


Fig. 2.— The light curve of Z Cam on the basis of AAVSO observations (from Warner 1995).

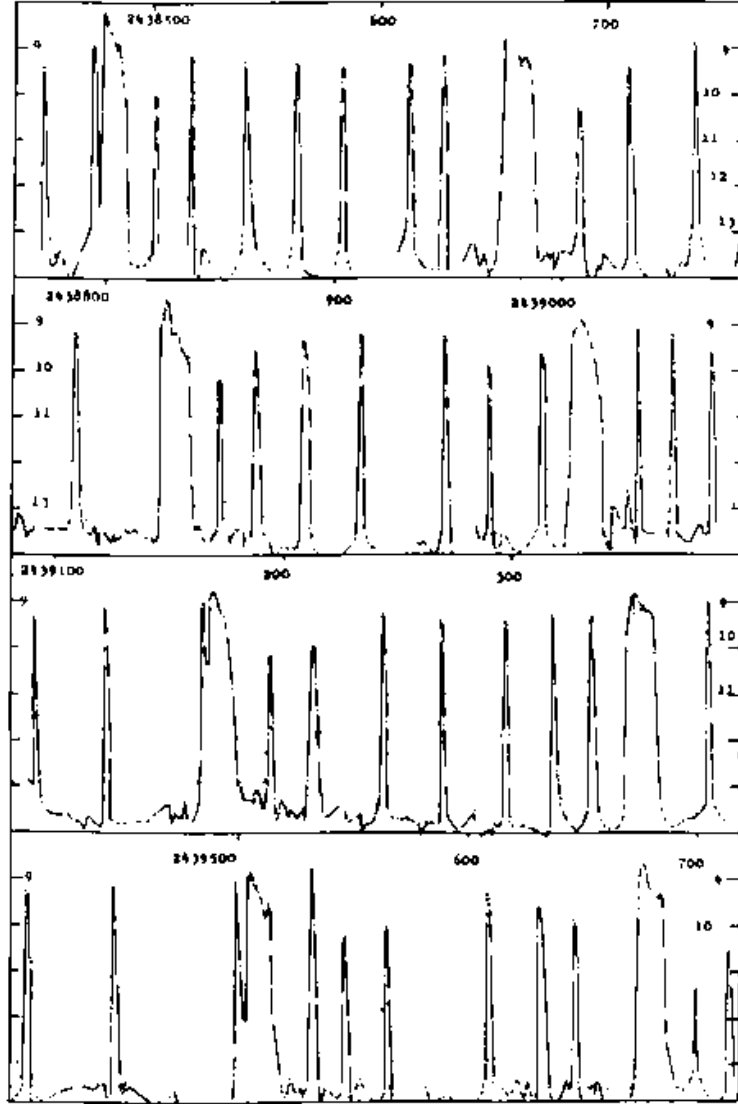


Fig. 3.— The light curve of VW Hya, exhibiting normal eruptions and superoutbursts (from Warner 1995).

conservation of angular momentum

$$\nu\Sigma\frac{d\Omega}{dR} = \Sigma V_R\Omega + \frac{\dot{M}(GM_*R_*)^{\frac{1}{2}}}{2\pi R^3} \quad (2)$$

conservation of energy

$$\frac{3GM_*\dot{M}}{8\pi R^3} \left[1 - \left(\frac{R_*}{R} \right)^{\frac{1}{2}} \right] = \sigma T_{eff}^4 \quad (3)$$

Here Σ is the disk surface density, V_R is the radial velocity, \dot{M} is the accretion rate, Ω is the angular velocity, ν is the kinematic viscosity and M_*, R_* are the mass and radius (respectively) of the central object. Combining equations (1) and (2) for a Keplerian flow gives

$$\nu\Sigma = \frac{\dot{M}}{3\pi} \left[1 - \left(\frac{R_*}{R} \right)^{\frac{1}{2}} \right] \quad (4)$$

Thus, approximately we have $\dot{M} \sim \nu\Sigma \sim T_{eff}^4$, a relation that will become useful later. Equations (1), (3), and (4) are normally augmented by a description of viscosity, which in the dimensional-analysis “ α prescription” (Shakura & Sunyaev 1973) is given by $\nu = \alpha c_s H$, where c_s is the speed of sound, H is the vertical disk half-thickness and α is a dimensionless parameter assumed to satisfy $\alpha \lesssim 1$ (see §2.5 and §3).

2.2. The Basic Local Limit Cycle

First, it is important to note that there are at least three fundamental timescales that are associated with standard accretion disks; dynamical, thermal and viscous. (A fourth timescale is associated with the propagation of transition fronts, see §2.4.) The dynamical time is the period of a Keplerian revolution. From hydrostatic equilibrium in the vertical direction, it is also the sound crossing time of the disk thickness (or the response time to a perturbation of vertical hydrostatics). The thermal timescale is the ratio of the thermal content to the local dissipation rate, and the viscous timescale is the time it takes material

to viscously drift inwards. These timescales are given by:

$$\begin{aligned} t_{dyn} &\sim \Omega^{-1} \sim \frac{R}{V_\phi} \sim \frac{H}{c_S} \\ t_{th} &\sim \frac{\Sigma c_S^2}{D(R)} \sim \frac{\Sigma c_S^2}{\nu \Sigma \Omega^2} \sim \frac{1}{\alpha} t_{dyn} \\ t_{vis} &\sim \frac{R^2}{\nu} \sim \frac{R^2}{\alpha c_S H} \sim \frac{1}{\alpha} \left(\frac{R}{H} \right)^2 t_{dyn} . \end{aligned} \quad (5)$$

Here $D(R)$ is the rate of viscous dissipation (per unit area) and all other symbols have their usual meaning. As we can see, since $\alpha \lesssim 1$ and in standard thin disks $H/R \ll 1$, in such disks $t_{dyn} < t_{th} < t_{vis}$.

The steady state equations (1), (3), and (4) are normally complemented by equations of hydrostatic equilibrium, mass conservation, and radiative transfer in the vertical direction. The computations of the local vertical structure (e.g. Meyer & Meyer-Hofmeister 1981; Cannizzo, Ghosh & Wheeler 1982; Smak 1982; Faulkner, Lin & Papaloizou 1983) were found to produce a multi-valued thermal equilibrium function in the $(\text{Log } T_{eff}; \text{Log } \Sigma)$ plane (see Fig. 4; from the discussion following eq. 4, T_{eff} can also be replaced by \dot{M} or $\nu\Sigma$). Note that this represents a local solution, at a given radial distance in the disk. The upper branch of the “S curve” corresponds to a hot, ionized state of the gas, while the lower branch corresponds to a cool, neutral state. It is easy to see that the lower and upper branches are stable (e.g. an increase in the surface density, which results in an increase in the viscous energy production rate, leads to an increase in the effective temperature, and concomitantly in the energy loss rate), while the middle branch is not. Imagine now that the rate at which mass is being transferred from the companion star is such that it corresponds to a point on the middle, unstable branch for some annulus (see Fig. 4). In such a case, no local stable equilibrium is possible. Rather, because the rate at which mass is being supplied is higher than the rate at which it can be transported locally, the surface density will increase (along the lower curve) until the critical surface density Σ_{max}

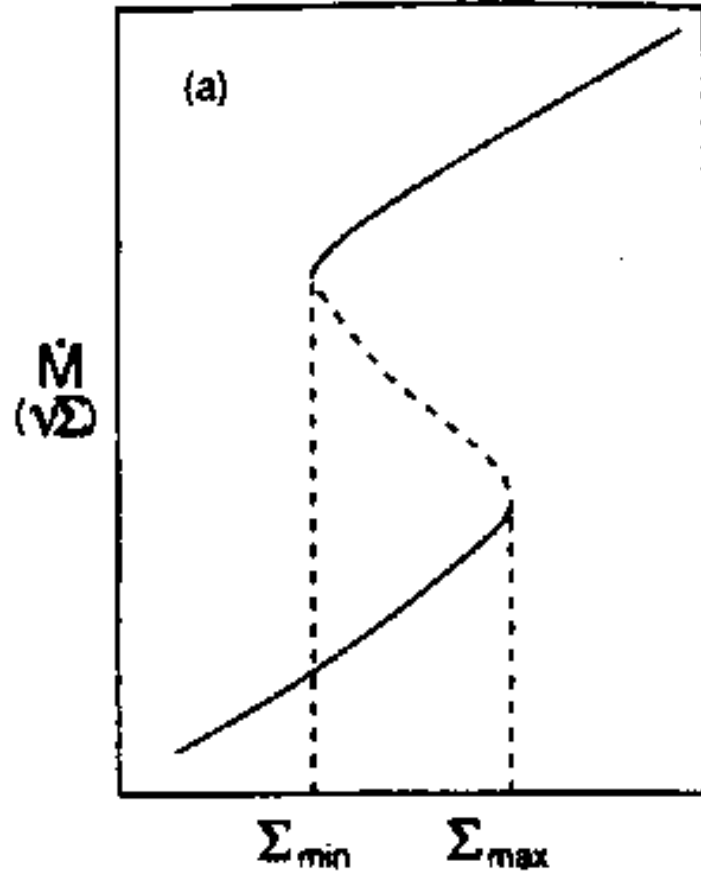


Fig. 4.— The S-shaped thermal equilibrium curve in the surface density-effective temperature plane (adapted from Osaki 1996).

is reached, at which point the annulus will heat up on a thermal timescale, “jumping” to the upper branch. There, since mass is being transported faster than it is being supplied, the surface density will decrease (along the upper curve) until the critical density Σ_{min} is reached. At that point the annulus will jump back to the lower branch, thus completing the limit cycle.

Before turning to time dependent evolution it is instructive to examine the physical reasons for the existence of such a multi-valued S-curve.

2.3. The S-Curve

The physical reason for the S-shaped equilibrium curve in the $(\nu\Sigma, \Sigma)$ (or (T_{eff}, Σ)) plane is the partial ionization of hydrogen at $T \sim 10^4$ K (e.g. Mineshige & Osaki 1983; Pojmanski 1986; Cannizzo 1992; Liu & Meyer-Hofmeister 1997).

This partial ionization produces two effects which give the S-curve its shape: (i) there is a steep dependence of the opacity on the temperature in the range $T \sim 6000$ – 10000 K (Fig. 5), which causes a change in the sign of $d\log(\nu\Sigma)/d\log\Sigma$, and (ii) the adiabatic temperature gradient drops substantially (Fig. 6), thus driving convection. Both of these effects produce a local maximum in $\log\Sigma$ as a function of $\log T_{eff}$ (Pojmanski 1986; Cannizzo 1992; See Fig. 7). Here, however, arises a difficulty which in my opinion has not been fully appreciated by disk instability modellers. While the opacity peak is hardly significant (e.g. in Fig. 7 it appears only for rather high ($\alpha \sim 1$), possibly unrealistic values of the viscosity parameter), it is the convection peak which determines the location, and to some extent the existence of the lower branch. This fact *raises serious doubts about the reality of the lower branch*. It should be realized that it appears almost certain now that angular momentum transport and energy dissipation in disks are governed by MHD

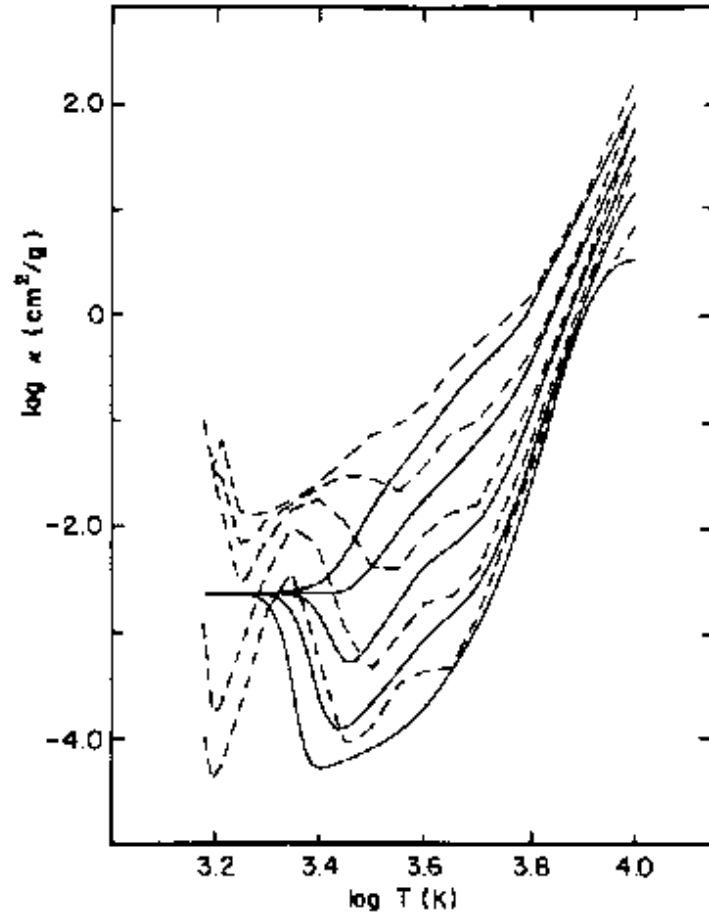


Fig. 5.— Rosseland mean opacities compiled by Cannizzo & Wheeler (1984).

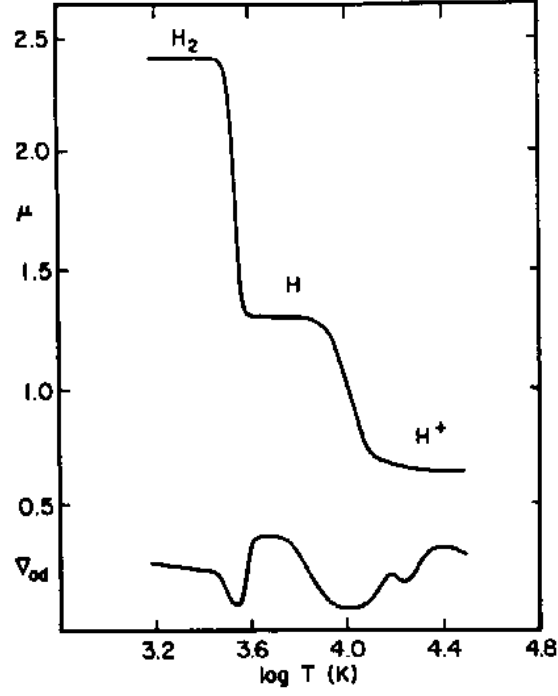


Fig. 6.— The mean molecular weight μ and the adiabatic index ∇_{ad} . Note the decrease in ∇_{ad} due to partial ionization (from Cannizzo & Wheeler 1984).

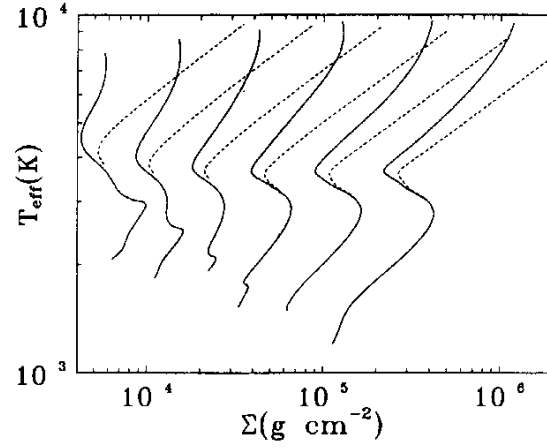


Fig. 7.— The effective temperature vs. surface density for (from left to right) $\log \alpha = 0.5$, 0, -0.5 , -1.0 , -1.5 and -2.0 . From Cannizzo (1992).

turbulence (e.g. Hawley, Gammie & Balbus 1996; Brandenburg, et al. 1995). Under these circumstances, and with the possibility that much of the energy dissipation occurs in a disk corona, the role of standard (mixing length) convection is questionable at best. I will return to this problem in §3.

2.4. Time Dependent Evolution

Many time-dependent simulations of the disk evolution have been carried out by a number of researchers; the most recent ones being by Cannizzo (1998), Hameury et al. (1998) and Menou, Hameury & Stehle (1998).

For the time-dependent case, the conservation equations can be written as:

mass conservation

$$\frac{\partial \Sigma}{\partial t} = -\frac{1}{r} \frac{\partial}{\partial r} (r \Sigma V_r) + \frac{1}{2\pi r} \frac{\partial \dot{M}_{tr}}{\partial r} \quad (6)$$

angular momentum conservation

$$\frac{\partial(\Sigma r^2 \Omega)}{\partial t} = -\frac{1}{r} \frac{\partial}{\partial r} (r^3 \Omega \Sigma V_r) + \frac{1}{r} \frac{\partial}{\partial r} \left(r^3 \nu \Sigma \frac{d\Omega}{d\Sigma} \right) + \frac{j_s}{2\pi r} \frac{\partial \dot{M}_{tr}}{\partial r} - \frac{1}{2\pi r} \tau_{tid}(r) \quad (7)$$

energy conservation

$$c_p \Sigma \frac{\partial T}{\partial t} = 2(Q^+ - Q^-) - 2 \frac{H}{r} \frac{\partial}{\partial r} (r F_r) - c_p V_r \Sigma \frac{\partial T}{\partial r} - \frac{\mathcal{R} T}{\mu} \frac{\Sigma}{r} \frac{\partial (r V_r)}{\partial r} \quad (8)$$

Here \dot{M}_{tr} is the rate at which mass is incorporated into the disk, j_s is the specific angular momentum of the stream from the inner Lagrangian point, τ_{tid} is the tidal torque applied by the secondary star, Q^+ and Q^- are the rates of heating and cooling (per unit area) respectively, and all other symbols have their usual meaning. While some small differences in the exact expressions used for the various terms exist among different researchers, these do not appear to be crucial for the general behavior.

The broad-brush evolution can be described as follows. In quiescence matter piles up in the disk, until at some radius the surface density exceeds Σ_{max} (Fig. 4). The corresponding annulus heats up on a thermal timescale. Since the viscosity increases with temperature (even for a constant α), this annulus starts to spread, thus initiating the propagation of heating fronts, which eventually bring the entire disk to a high state (the upper branch). A typical evolution of the surface density, the accretion rate onto the central object and the disk mass is shown in Fig. 8 (taken from Mineshinge & Osaki 1985 and Cannizzo, Wheeler & Polidan 1986). Two cases are shown; one in which the outburst begins at a large radius, and one in which it begins at a small radius. As can be seen in the figures, since most of the disk mass lies in the outer parts of the disk, outbursts starting from the outside produce a much steeper increase in the accretion rate. Since in the high state $\Sigma(r) \sim r^{-1}$, while $\Sigma_{min} \sim r$, it is always the case that Σ first drops below Σ_{min} at the outer disk radius. This initiates the propagation of a cooling front which transforms the entire disk to a low state configuration, thus terminating the outburst. In cases in which the cooling front cannot propagate (e.g. due to strong irradiation of the disk by the central source), the evolution is slower, because it has to proceed on the viscous timescale. This may produce flat-topped maxima in the light curve.

The structure and physical properties of the transition fronts have been studied extensively both analytically and numerically (e.g. Meyer 1984; Papaloizou & Pringle 1985; Lin, Papaloizou & Faulkner 1985; Cannizzo, Chen & Livio 1995; Vishniac & Wheeler 1996; Vishniac 1997; Menou, Hameury & Stehle 1998). Broadly speaking, these works have shown that the speed of the fronts is of the order of $V_F \sim \alpha_H c_S$, where α_H is the viscosity parameter in the hot state (see below) and c_S is the speed of sound in the front (for a more detailed discussion see Vishniac 1997). The width of the front was found by Menou et al. (1998) to be proportional to the disk pressure scale height H .

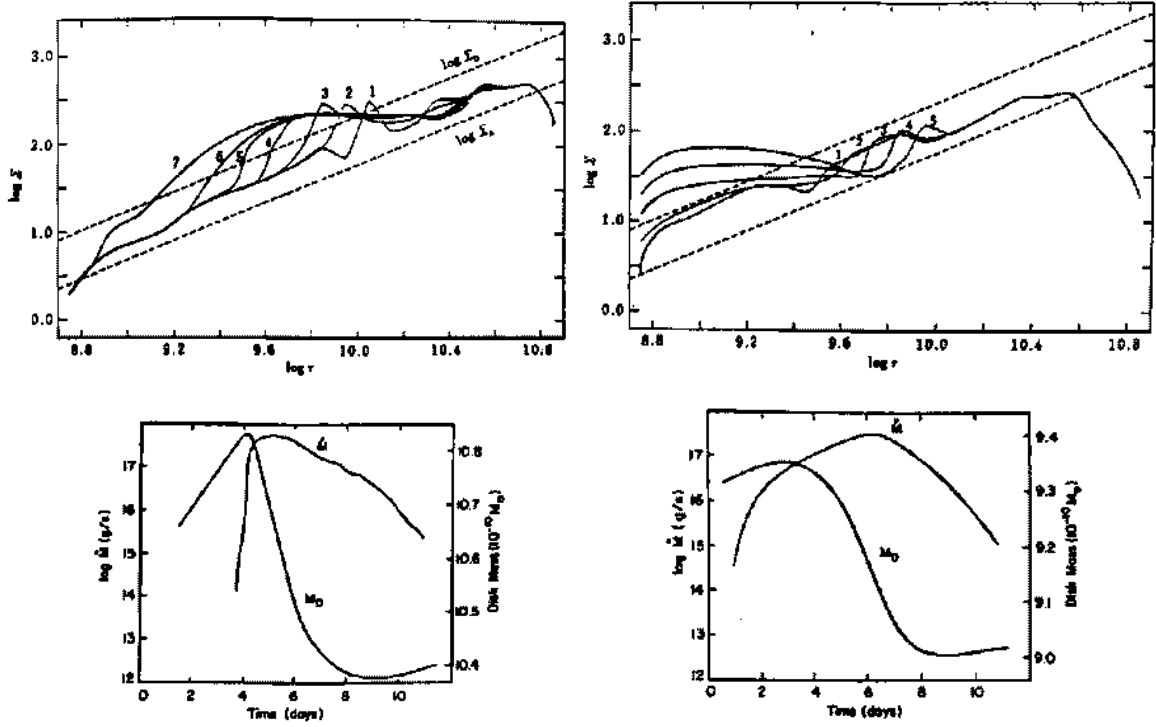


Fig. 8.— The left two figures (8a) show how the disk responds to an outburst which begins at a large radius. The right two figures (8b) show an outburst starting at a small radius. The top figures show the evolution of the surface density, the bottom two figures show the accretion rate and the disk mass (adapted from Cannizzo 1993).

2.5. Viscosity

Angular momentum transport in accretion disks is due to magnetically driven turbulence (e.g. Balbus & Hawley 1998; Godon & Livio 1998 and references therein). Consequently, expressing the anomalous viscosity by means of a fixed parameter does not represent adequately the physical situation. The following discussion should be viewed therefore as a time and space overaging of the process of angular momentum transport. Since the MHD simulations indicate that Maxwell stresses dominate over Reynolds stresses (e.g. Hawley et al. 1996), the viscosity parameter α is given by the appropriately overaged value of $B_R B_\phi / 4\pi \rho c_S^2$, where B_R and B_ϕ are the radial and toroidal (respectively) components of the dynamo-generated magnetic field.

From disk instability models of dwarf nova eruptions, it was generally found that in order to reproduce the observed amplitudes and timescales one needs to assume that the viscosity parameter in the hot state, α_H , is larger than the one in the cold state, α_C , by a factor of 5–10 (e.g. Smak 1984). Otherwise, only relatively frequent, small oscillations in the luminosity are produced. The changes to a local S-curve, introduced by using $\alpha_H/\alpha_C \sim 5$ instead of a constant value, are shown in Fig. 9 (Hameury et al. 1998).

One may ask, do we have any observational handle on the value of α ?

From visual amplitudes and rates of decline (when compared to models) one obtains $\alpha_H \sim 0.2$ (Smak 1984). On the other hand, Livio & Spruit (1991) have shown that from the recurrence times of dwarf nova eruptions one obtains $\alpha_C \lesssim 0.05$ (see also Smak 1996).

2.6. A Representative Model Calculation

The most recent, extensive numerical models have been carried out by Hameury et al. (1998). Unlike in some of the previous calculations, these authors use an adaptive grid

technique and an implicit numerical scheme, which allows them to resolve the transition fronts. Hameury et al. also allow the outer disk radius to vary—a boundary condition which proves to be important for the obtained behavior (see below). The results of two typical calculations are shown in Figs. 10–11, for two values of the accretion rate. The main difference between the two calculations is the fact that for the higher mass transfer rate ($\dot{M} = 10^{17} \text{ gs}^{-1}$) the eruption is “outside-in” (namely, starts at a large radius with the transition front propagating inwards; these are also known as “type A” outbursts, Smak 1987), while for the lower ($\dot{M} = 10^{16} \text{ gs}^{-1}$) it is “inside-out” (type B). This basic difference in the behavior is well understood. In the case of a high mass transfer rate, material accumulates in the outer disk faster than it drifts inwards, hence the surface density first exceeds the local Σ_{max} in the outer part. For relatively low accretion rates Σ_{max} is first exceeded in the inner disk. The obtained behavior of the disk radius agrees well with observations (e.g. Smak 1984; O’Donoghue 1986). As the outburst is initiated and material starts to be accreted, it transports its angular momentum outwards, thus the outer radius expands (Livio & Verbunt 1988).

As I noted above, Hameury et al. examined the effects of using as an outer boundary condition a disk radius, R_{out} , that is allowed to vary (see also Ichikawa & Osaki 1992; Livio & Verbunt 1988), as opposed to a fixed R_{out} . They found that when R_{out} was kept fixed, the outbursts always tended to be inside-out, and they involved the accretion of a larger fraction of the disk mass. The reason for the latter behavior is easy to understand. When R_{out} is fixed, the material that moves outward (with the angular momentum it absorbed) piles up at the outer edge increasing there the surface density. Consequently, all of that material needs to be accreted before the surface density drops below Σ_{min} and the cooling wave is initiated. The light curves obtained under the two different boundary conditions are shown in Fig. 12.

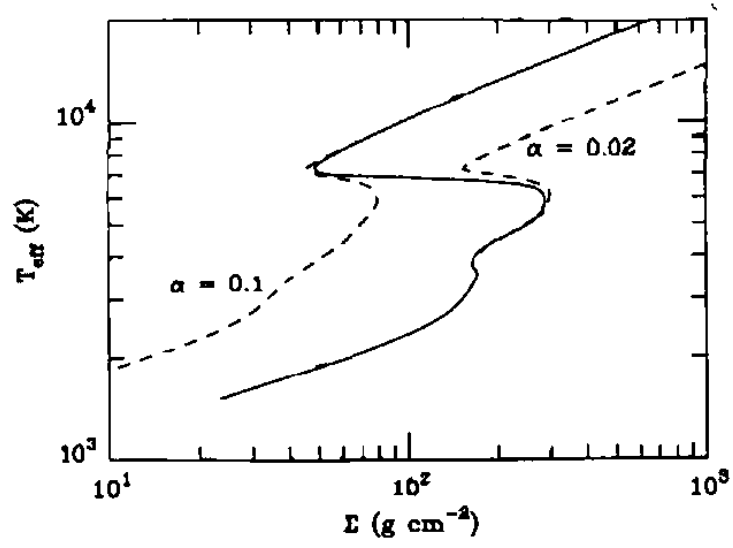


Fig. 9.— The dashed S-curves correspond to constant α , $\alpha = \alpha_H$ (left) and $\alpha = \alpha_C$ (right). The solid line represents $\alpha = \alpha_H$ on the upper branch and $\alpha = \alpha_C$ on the lower branch (from Hameury et al. 1998).

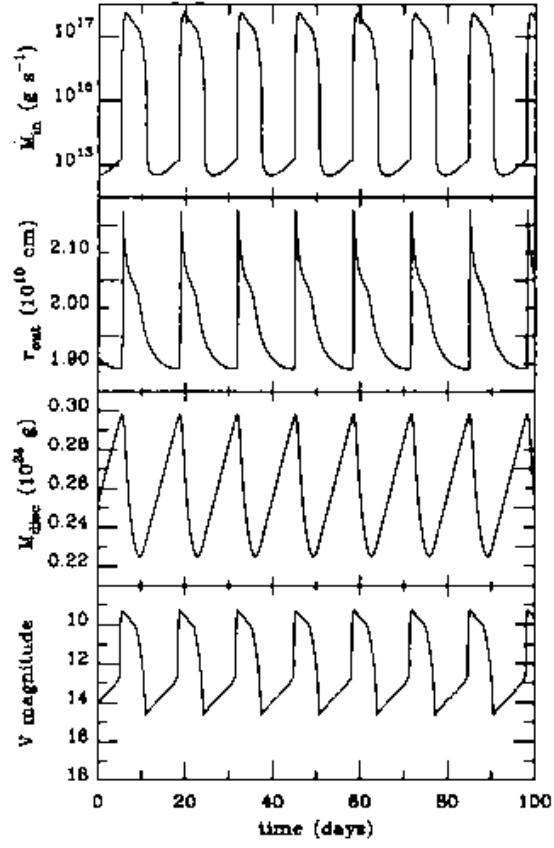


Fig. 10.— The outbursts obtained for $M_{WD} = 0.6 M_{\odot}$, $\alpha_C = 0.04$, $\alpha_H = 0.2$ and $\dot{M} = 10^{17} \text{ gs}^{-1}$ (from Hameury et al. 1998).

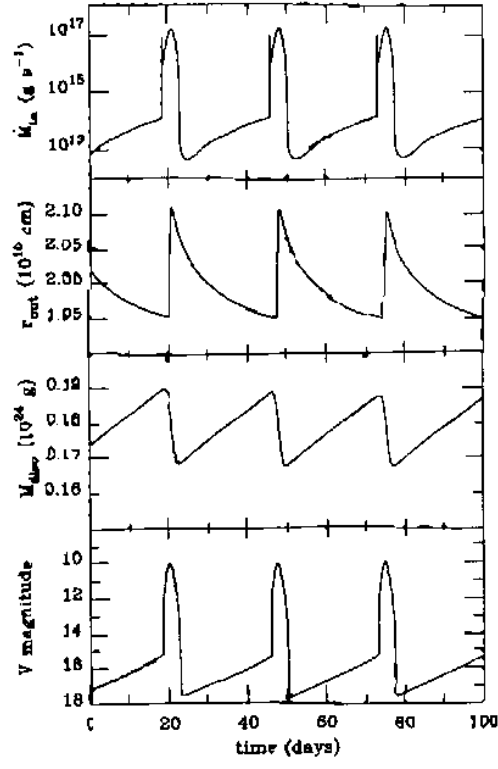


Fig. 11.— The same as Fig. 10, for $\dot{M} = 10^{16} \text{ gs}^{-1}$.

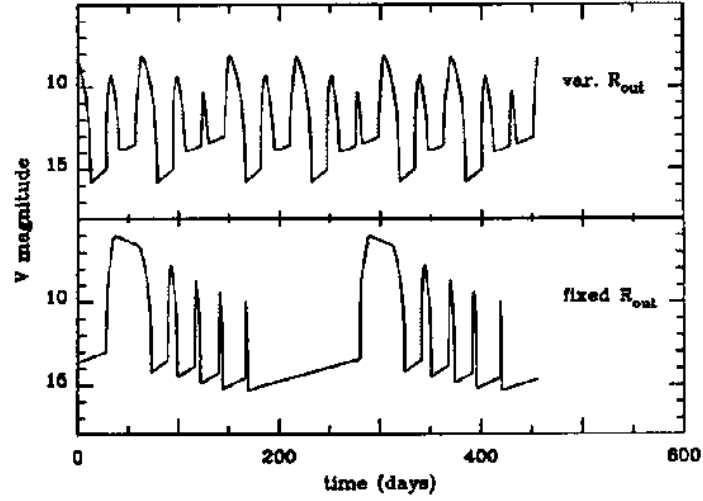


Fig. 12.— The light curves that are obtained assuming a fixed outer disk radius (lower panel), and allowing the outer radius to vary (upper panel). From Hameury et al. (1998).

I should note that in addition to successfully reproducing light curves and the behavior of the disk radius, the disk instability model has provided a reasonable explanation for the observed distribution of systems in stability/instability regions in the (\dot{M}, P_{orb}) plane (where P_{orb} is the binary orbital period; e.g. Smak 1989; Osaki 1996). In particular, the Z Cam objects which experience “standstills” (Fig. 2) are found to be right at the border between the unstable and stable regions. Thus, it is expected that small changes in \dot{M} can carry them into and out of the instability region, which can account for the standstills.

3. MHD Turbulence and Limit Cycles

Since angular momentum transport in accretion disks is driven by MHD turbulence, it is appropriate to ask whether the thermal limit cycle model as described in the previous sections is consistent with such a dynamo-generated “viscosity.” In particular, it is important to attempt to understand what could cause the existence of two values for the viscosity parameter, namely α_H and α_C . In this respect, the following *suggestion* has been made (Armitage, Livio & Pringle 1996; Gammie & Menou 1998): *the MHD turbulence is quenched in quiescence, leading to a low viscosity, while it is operative in outburst, leading to a high viscosity.*

The exact mechanism by which the MHD turbulence is suppressed is not clear at the moment, but there exist at least two possibilities: (i) when the disk cools, the magnetic field does not decay as fast (it decays on a superthermal timescale, e.g. Tout & Pringle 1992). Consequently, the condition for magnetorotational instability (Balbus & Hawley 1991), $B_z^2 < 24/\pi\rho c_S^2$, is violated, and hence the dynamo action is suppressed. (ii) When the disk cools, the magnetic Reynolds number $Re_M = c_S H/\eta$ (where η is the resistivity) can decrease below $\sim 10^4$. Numerical simulations indicate that the MHD turbulence may be suppressed when $Re_M \lesssim 10^4$ (Hawley, Gammie & Balbus 1996).

While I am slightly more inclined to favor the second possibility, the important thing for the present discussion is the fact that viscosity is decreased in quiescence as a result of cooling.

If viscosity in quiescence is indeed low, this should have some obvious observational consequences: (i) little accretion should take place in quiescence. (ii) There should be little or no emission from the boundary layer and little UV emission from the inner disk. (iii) The temperature profile in quiescence should be very different from that of a standard disk (it should basically be flat). (iv) A UV delay (with respect to optical) should be observed in the rise to outburst.

There are strong indications that all of these predictions are consistent with observations at least in some systems. For example, observations of all of the black hole transients show very low accretion in quiescence. Similarly, observations of the cataclysmic variables OY Car and Z Cha indicate that the accretion rate in the inner disk is lower by about a factor of 100 than that in the outer disk (e.g. Wood et al. 1986, 1989). Also, the temperature profile in OY Car is extremely flat in quiescence, while it is consistent with that of a standard disk in Z Cha in outburst.

It therefore appears that there is some merit to the suggestion that the viscosity in quiescence is low. However, an important question arises, if material accumulates more or less in a ring (due to the low viscosity), *how can inside-out (type B) outbursts be obtained?* Before I attempt to answer this question it is important to examine the observational evidence that inside-out outbursts do indeed exist. There are by now 15 dwarf novae with claimed positively identified outburst types (e.g. Smak 1996; Warner 1995, Table 3.6). Outside-in outbursts are characterized by a *rapid rise*, the existence of a *UV delay*; and they follow a *broad loop* in a color-color diagram. All of these properties follow directly from the fact that the outburst starts from the outer disk, where most of the mass is concentrated

(see §2.6). Examples for such outbursts can be seen in VW Hyi (Smak 1987; Fig. 13) and they are well reproduced in theoretical models. Inside-out outbursts are characterized by a *slower rise*, *no UV delay*, and a *narrow loop* in the color-color diagram (Fig. 13). All of these, in turn, are a consequence of the fact that the outburst starts in the inner part of the disk, where there is relatively little mass. Examples to this type of outburst are seen in SS Cyg and AH Her, and again they are adequately reproduced by models. One can therefore conclude with some certainty that outbursts of the two types do exist.

I now return to the question of how can inside-out outbursts be reconciled with the suggestion of low viscosity at quiescence. In particular, I note the following, seemingly strange fact (e.g. Warner 1987): SU UMa systems show *only* outside-in outbursts while Z Cam systems show *only* inside-out outbursts, in spite of the fact that the accretion rate in Z Cam systems is more than ten times higher than in SU UMa systems!

I would like to suggest the following possible solution. If we take as the critical (for suppression of MHD turbulence) magnetic Reynolds number $Re_M^{crit} \sim 10^4$, then it can be shown (e.g. Gammie & Menou 1998) that the critical temperature corresponding to this value (so that for $T > T_{crit}$, $Re_M > Re_M^{crit}$) is approximately given by

$$T_{crit} \sim 7400\text{K } \Omega^{0.2} \Sigma^{0.038} . \quad (9)$$

It can easily be shown then that the condition $T > T_{crit}$ assumes the form $\xi \gtrsim \text{const.}$, with

$$\xi = \left(\frac{\dot{M}}{P_{orb}} \right)^{0.3} f^{-\frac{3}{4}}(q) , \quad (10)$$

where P_{orb} is the orbital period and $f(q)$ is some function of the mass ratio of the two binary components. Now, it turns out that $\xi_{Z\text{ Cam}} \sim 2\xi_{SU\text{ UMa}}$. Therefore, it is possible that the disk has a non-negligible viscosity in quiescence in Z Cam (and similar) systems and no viscosity in systems like SU UMa. This could resolve the puzzle of inside-out outbursts.

I therefore propose as a possibility the following new scenario for dwarf nova eruptions

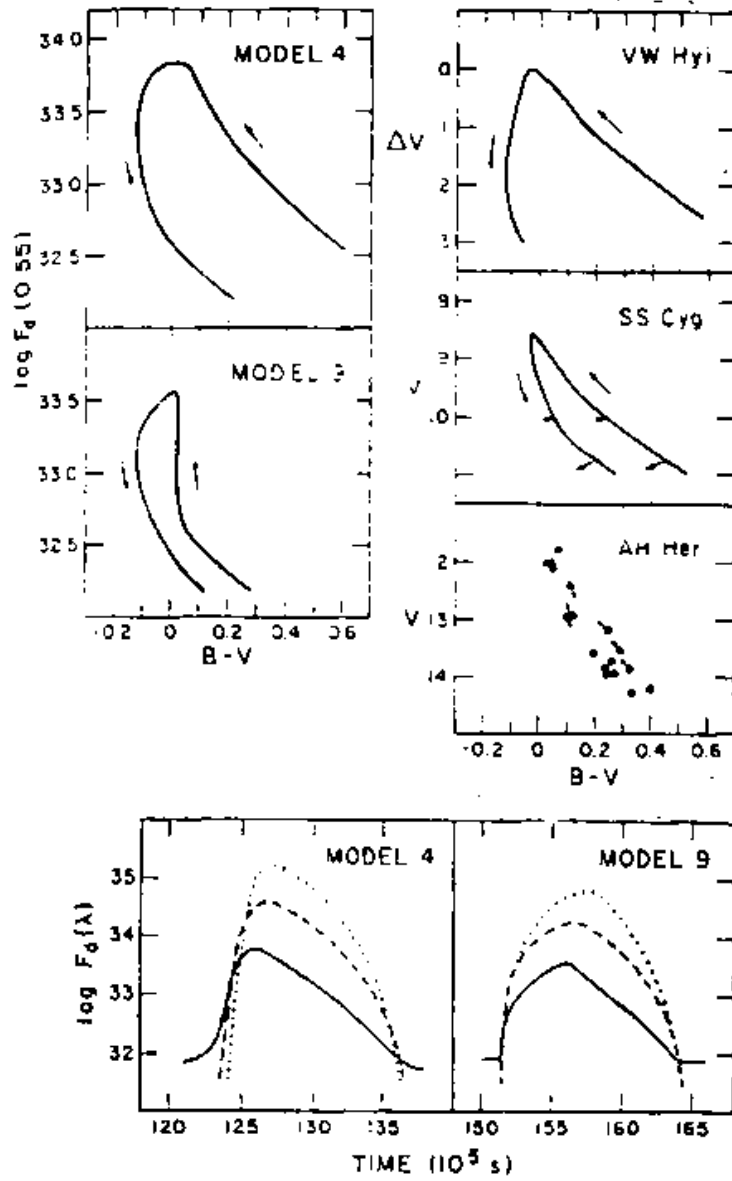


Fig. 13.— Examples of observations and model calculations showing a rapid rise and a broad loop in the color-color diagram for outside-in outbursts, and a slower rise and a narrow loop in the color-color diagram for inside-out outbursts (adopted from Smak 1987).

(see also Armitage, Livio, & Pringle 1996; Gammie & Menou 1998). In the disks of systems in which at quiescence $Re_M \ll Re_M^{crit}$ (or some equivalent condition for the suppression of MHD turbulence), there is essentially no viscosity at quiescence. These systems experience outside-in outbursts. The initiation of these outbursts may be aided by the ring of accumulated material becoming unstable to the Papaloizou-Pringle (1994) instability (e.g. Rozyczka & Spruit 1993).

In the disks of systems in which at quiescence $Re_M \gtrsim Re_M^{crit}$ (or an equivalent condition allowing MHD turbulence), accretion takes place also in quiescence. In such systems the possibility for inside-out eruptions exists. The main implication of this new scenario is that *a “standard” lower branch of the S-curve may not exist*. This would be consistent with the doubts I raised about the existence of such a branch in §2.3. It is clear that the viscosity cannot be zero at quiescence in all systems, since some systems (e.g. HT Cas, WX Hyi) exhibit low states which are almost certainly associated with a reduction in \dot{M} (these low states would not have been seen if there was no viscosity).

4. Superhumps and Superoutbursts

I would like now to discuss briefly another disk instability, the one producing superoutbursts and superhumps. Superhumps are periodic photometric humps that are observed in some dwarf nova systems, and they have periods that are longer by a few percent than the orbital period (Fig. 14; see e.g. Osaki 1996; Warner 1995 for reviews of their properties). Most of the systems that exhibit superhumps (the SU UMa systems) have orbital periods below the 2–3 hr period gap in the distribution of cataclysmic variables (TU Men is an exception). Some black hole soft x-ray transients also apparently exhibit superhumps (O’Donoghue & Charles 1996). In the SU UMa systems, superhumps are observed mostly during superoutbursts (see below), although in some systems (like

V1159 Ori) they have been observed after superoutbursts (e.g. Patterson et al. 1995).

Superoutbursts are eruptions that are brighter than normal by about 0.7 mag, and longer than normal by a factor of 5–10 (Fig. 3). The general impression is that superoutbursts start with normal outbursts (e.g. Vogt 1974; Warner 1995).

The basic model for superhumps has been suggested by Whitehurst (1988), and further investigated by Hirose & Osaki (1990) and Lubow (1991). It involves a tidally driven eccentric instability of the accretion disk. The eccentric disk precesses at a period P_{prec} . The superhump period is identified as the synodic period between the precessing eccentric disk and the orbital period

$$\frac{1}{P_{SH}} = \frac{1}{P_{orb}} - \frac{1}{P_{prec}} \quad . \quad (11)$$

Non-axisymmetric waves in the disk can be expressed in the form $\exp[i(k\theta - \ell\Omega t)]$ (where $\theta = \phi + \Omega t$, with ϕ being the azimuthal angle in the corotating frame). The modes are thus identified by the pair (k, ℓ) . Hirose & Osaki (1990) and in particular Lubow (1991) demonstrated the crucial role played by the 3:1 resonance in the disk in the excitation of the eccentric instability (see also Whitehurst & King 1991; Molnar & Kobulnicky 1992). Very briefly, a perturbation in the eccentricity (characterized by (1,0)) combines with the resonant effect of the 3:1 resonance in the tidal potential (corresponding to (3,3)) to produce a two-armed spiral density wave (characterized by (2,3)). This spiral wave ((2,3)), in turn, combines again with the tidal potential ((3,3)) to amplify the eccentricity ((1,0)). For the instability to grow, the 3:1 resonance radius must lie within the disk. This implies that this instability can occur only for mass ratios satisfying $q = m_2/m_1 \lesssim 0.25$. This explains the fact that superhumps are found primarily below the period gap or in black hole x-ray binaries.

Surprisingly, it has proven much more difficult to find a convincing model for the superoutbursts. The history of the field is nicely summarized in Warner (1995) and Osaki

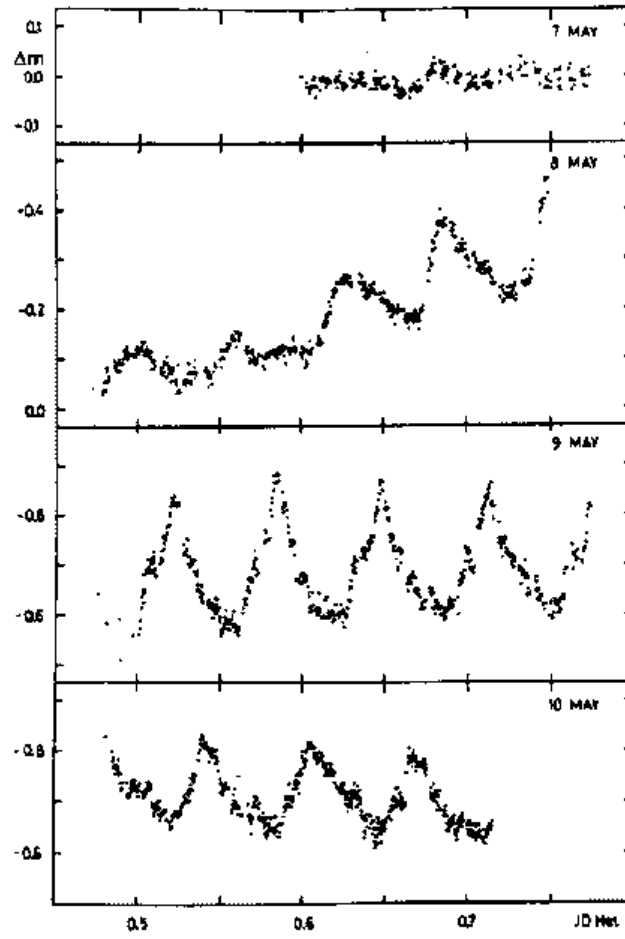


Fig. 14.— The development of superhumps in V436 Cen. From Semeniuk (1980).

(1996). The most promising model has been suggested by Osaki (1989). In this model, the following sequence of events is suggested to occur. As the accretion disk undergoes normal dwarf nova eruptions, in each outburst the mass that is actually accreted onto the white dwarf is smaller than the mass accumulated (via transfer) during the inter-outburst period. This agrees with the results of detailed simulations (e.g. Cannizzo 1993). Consequently, both the mass and the angular momentum of the disk are building up gradually, and the disk radius experiences a slow overall increase with each successive eruption (Fig. 15).

At some point, the disk radius hits the 3:1 resonance and the tidally induced eccentric instability sets in, producing a precessing eccentric disk. Osaki *assumed* that the eruption that ensues at that point results in an *enhanced* rate of removal of angular momentum by the tidal interaction (compared to normal outbursts), so that a much larger fraction of the disk mass is accreted, thus producing a superoutburst. Until recently, all of the suggestions in Osaki’s model have been verified by numerical simulations, except the assumption about an increased rate of removal of angular momentum. Most recently however, a simulation by Murray (1998) showed that this assumption is likely to be correct too. Murray simulated normal outbursts by an increased viscosity and showed that once the disk encounters the 3:1 resonance it becomes tidally unstable and the tidal torques become much more efficient in removing angular momentum from the disk. He further showed that the resulting increased accretion rate is consistent with superoutbursts.

5. Tentative Conclusions

In recent years it appeared as if the question of dwarf nova eruptions has been fully solved, maybe with just a few details left to be sorted out. On the other hand, on the question of superoutbursts considerable skepticism existed in relation to Osaki’s model. The enormous progress in the understanding of angular momentum transport in accretion

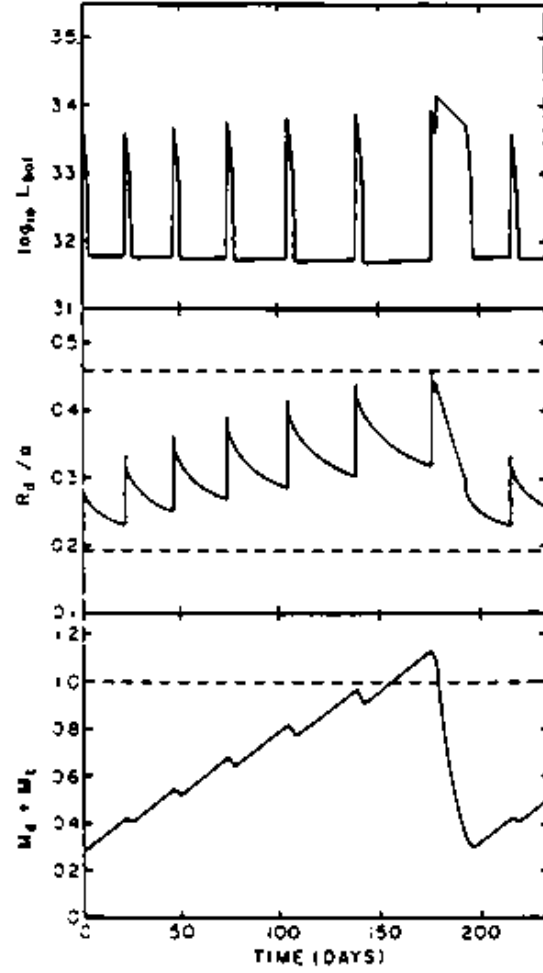


Fig. 15.— The time evolution of the accretion disk luminosity, radius, and mass (from top to bottom) in a simplified thermal-tidal instability model for superoutbursts (from Osaki 1996).

disks on one hand, and the increased sophistication of numerical simulations on the other, have contributed to a renewed interest in both of these problems.

On the basis of the material presented in the previous sections I am inclined to make the following tentative suggestions:

(1) Dynamo generation of viscosity may be suppressed in some systems (and reduced in others) in quiescence, due to cooling. The difference in the angular momentum transport properties may be the main cause for dwarf nova eruptions and x-ray transient outbursts.

A continuing serious effort will be required, in MHD simulations on one hand, and in observations of systems in quiescence on the other, to determine the viability of the above suggestion.

(2) Superoutbursts are probably caused by a thermal-tidal instability, as has been proposed by Osaki (with the normal outbursts however occurring as in (1) above).

The best observational test of this model can be provided by *monitoring the behavior of the disk radius* through a series of normal outburst and a superoutburst.

This work has been supported by NASA Grant NAG5-6857. I thank the Isaac Newton Institute for Mathematical Sciences for its hospitality and John Cannizzo and Kristen Menou for helpful discussions.

REFERENCES

- Armitage, P. J., Livio, M. & Pringle, J. E. 1996, *ApJ*, 457, 332
- Balbus, S. A. & Hawley, J. F. 1991, *ApJ*, 376, 214
- Balbus, S. A. & Hawley, J. F. 1998, *Rev. Mod. Phys.*, 70, 1
- Brandenburg, A., Nordland, A., Stein, R. F. & Torkelsson, U. 1995, *ApJ*, 446, 741
- Cannizzo, J. K. 1992, *ApJ*, 385, 94
- Cannizzo, J. K. 1993, in *Accretion Disks in Compact Stellar Systems*, ed. J. C. Wheeler (Singapore: World Scientific), p. 6
- Cannizzo, J. K. 1998, *ApJ*, 494, 366
- Cannizzo, J. K., Ghosh, P. & Wheeler, J. C. 1982, *ApJ*, 260, L83
- Cannizzo, J. K. & Mattei, J. 1992, *ApJ*, 401, 642
- Cannizzo, J. K. & Wheeler, J. C. 1984, *ApJS*, 55, 367
- Cannizzo, J. K., Wheeler, J. C. & Polidan, R. S. 1986, *ApJ*, 301, 634
- Chen, W., Shrader, C. R. & Livio, M. 1997, *ApJ*, 491, 312
- Faulkner, J., Lin, D. N. C. & Papaloizou, J. 1983, *MNRAS*, 205, 359.
- Gammie, C. F. & Menou, K. 1998, *ApJ*, 492, L75
- Godon, P. & Livio, M. 1998, *ApJ*, submitted
- Hameury, J.-M., Menou, K., Dubus, G., Lasota, J.-P. & Huré, J.-M. 1998, *MNRAS*, in press, astro-ph/9803242
- Hawley, J., Gammie, C. F. & Balbus, S. 1996, *ApJ*, 464, 690
- Hirose, M. & Osaki, Y. 1990, *PASJ*, 42, 135
- Ichikawa, S. & Osaki, Y. 1992, *PASJ*, 44, 15

- Lasota, J.-P. & Hameury, J.-M. 1998, in *Accretion Processes in Astrophysics—Some Like it Hot*, eds. S. Holt & T. Kallman, in press, astro-ph/9712202
- Lin, D. N. C., Papaloizou, J. C. B. & Faulkner, J. 1985, MNRAS, 212, 105
- Liu, B. F. & Meyer-Hofmeister, E. 1997, A&A, 328, 243
- Livio, M. & Spruit, H. C. 1991, A&A, 252, 189
- Livio, M. & Verbunt, F. 1988, MNRAS, 232, 1p
- Lubow, S. 1991, ApJ, 381 259
- Menou, K., Hameury, J.-M. & Stehle, R. 1998, MNRAS, in press
- Meyer, F. 1984, A&A, 131, 303
- Meyer, F. & Meyer-Hofmeister, E. 1981, A&A, 104, L10
- Mineshige, S. & Osaki, Y. 1983, PASJ, 35, 377
- Molnar, L. A. & Kobulnicky, H. A. 1992, ApJ, 392, 678
- Murray, J. R. 1998, MNRAS, 297, 323
- O’Donoghue, D. 1986, MNRAS, 220, 23p
- O’Donoghue, D. & Charles, P. A. 1996, MNRAS, 282, 191
- Osaki, Y. 1989, PASJ, 41, 1005
- Osaki, Y. 1996, PASP, 108, 39
- Papaloizou, J. C. V. & Pringle, J. E. 1985, MNRAS, 217, 387
- Papaloizou, J. C. B. & Spruit, H. C. 1993, ApJ, 417, 677.
- Patterson, J., Jablonsky, F., Koen, C., O’Donoghue, D. & Skillman, D. R. 1995, PASP, 107, 1183
- Pojmanski, G. 1986, Acta Astron., 36, 69

- Pringle, J. E. 1981, *ARA&A*, 19, 137
- Rozyczka, M. & Spruit, H. C. 1993, *ApJ*, 417, 677
- Semeniuk, I. 1980, *A&AS*, 39, 29
- Shakura, N. I. & Sunyaev, R. A. 1973, *A&A*, 24, 337
- Smak, J. 1984, *Acta Astr.*, 34, 93
- Smak, J. 1987, *A&SS*, 131, 497
- Smak, J. 1996, in *Cataclysmic Variables and Related Objects*, eds. A. Evans, & J. H. Wood (Dordrecht: Kluwer), p. 45
- Tout, C. A. & Pringle, J. E. 1992, *MNRAS*, 259, 604
- Vishniac, E. T. 1997, *ApJ*, 482, 414
- Vishniac, E. T. & Wheeler, J. C. 1996, *ApJ*, 471, 921
- Vogt, N. 1974, *A&A*, 36, 369
- Warner, B. 1987, *MNRAS*, 227, 23
- Warner, B. 1995, *Cataclysmic Variable Stars* (Cambridge: Cambridge University Press)
- Whitehurst, R. 1988, *MNRAS*, 232, 35
- Whitehurst, R. & King, A. 1991, *MNRAS*, 249, 25
- Wood, J., Horne, K., Berriman, G., Wade, R., O’Donoghue, D., & Warner, B. 1986, *MNRAS*, 219, 629
- Wood, J. H. et al. 1989, *MNRAS*, 239, 809